Received: 30 August 2016 | Accepted: 13 March 2017

DOI: 10.1002/hyp.11174

WILEY

RESEARCH ARTICLE

Quantification of uncertainty in the assessment of future streamflow under changing climate conditions

Sohom Mandal | **Slobodan P. Simonovic**

Facility for Intelligent Decision Support, Spencer Engineering Building, Department of Civil and Environmental Engineering, Western University, London, ON N6A 5B9, Canada

Correspondence
Sohom Mandal, Facility for Intelligent Decision Support, Spencer Engineering Building, Department of Civil and Environmental Engineering, Western University, London, ON N6A 5B9, Canada.
Email: sohomiitb@gmail.com

Funding Information
Natural Sciences and Engineering Research Council of Canada, Grant/Award Number: Discovery Grant: CRDPJ462879-13

Abstract

Climate change has a significant influence on streamflow variation. The aim of this study is to quantify different sources of uncertainties in future streamflow projections due to climate change. For this purpose, 4 global climate models, 3 greenhouse gas emission scenarios (representative concentration pathways), 6 downscaling models, and a hydrologic model (UBCWM) are used. The assessment work is conducted for 2 different future time periods (2036 to 2065 and 2066 to 2095). Generalized extreme value distribution is used for the analysis of the flow frequency. Strathcona dam in the Campbell River basin, British Columbia, Canada, is used as a case study. The results show that the downscaling models contribute the highest amount of uncertainty to future streamflow predictions when compared to the contributions by global climate models or representative concentration pathways. It is also observed that the summer flows into Strathcona dam will decrease, and winter flows will increase in both future time periods. In addition to these, the flow magnitude becomes more uncertain for higher return periods in the Campbell River system under climate change.

KEYWORDS

climate change, downscaling, hydrologic model, streamflow, uncertainty

1 | INTRODUCTION

Impacts of climate change possess a significant threat to the water resources for all continents in the world. Changing climate will magnify the existing risks and increase the future risks associated with management of water resources systems. The frequency and magnitude of streamflow are affected by climate change, and there is a clear indication that changes in streamflow will continue in the future because of continuous increase in the concentration of greenhouse gasses (GHGs) in the atmosphere (IPCC, 2013). The streamflow variation is not uniform across the world, but it is hydrologic regime specific. For example, a decreasing trend in maximum flows has been identified for the maritime provinces of Canada (east coast) and the St Lawrence River basin (Leclerc & Ouarda, 2007) in the last two decades. On the contrary, in the northwest and west parts of Canada, an increasing trend in minimum annual flow has been observed for the period of 1970–2005 (Warren & Lemmen, 2014). Variation in magnitude and frequency of streamflow increases the vulnerability of the water infrastructure. According to the Public Infrastructure Engineering Vulnerability Committee of Engineers Canada (Canadian Council of Professional Engineers, 2008), failure of water resource's infrastructures due to extreme hydrological events (droughts and floods) will increase across Canada due to climate change. A study by the Canadian Institute of Actuaries (2014) found that water-related insured damage and losses could increase by about 20% to 30% in the next few decades across Canada. Simonovic (2008) also suggested that water resource infrastructure planning, design, and operations should be revised to accommodate the expected changes in magnitude and frequency of streamflows.

Atmosphere–Ocean global climate models (AOGCMs) are credible and reliable tools for global scale climate analyses. These models are numerical representation of the earth's climate system, which includes

Acronyms: AOGCM, Atmosphere–Ocean global climate model; BC, British Columbia; BCCAQ, bias correction constructed analogues with quantile mapping reordering; BCSD, bias-corrected spatial disaggregation; BR, beta regression; CMIP5, Coupled Model Intercomparison Project 5; DSM, downscaling model; GCM, global climate model; GEV, generalized extreme value; GHG, greenhouse gas; GWh, Gigawatt hours; hus, specific humidity; IDW, inverse distance weighting; IPCC, Intergovernmental Panel on Climate Change; K-NN, k-nearest neighbors; KR, Kernel regression; MEB, maximum entropy bootstrap; mslp, mean sea level pressure; NSE, Nash–Sutcliffe efficiency; Pr, precipitation; RCPs, representative concentration pathways; RSME, root mean square error; Tmax, maximum temperature; Tmin, minimum temperature; UBCWM, UBC watershed model

biological, chemical, and physical properties of climate variables and feedback relationships between these variables. Because AOGCMs provide information on global scale, tools are required for regional studies to convert the global scale information to local scale. Downscaling methods are well known and used for transferring coarse-scale climate information to regional scale. Projection of hydro-climatic variables using downscaling includes several sources of uncertainties. Uncertainties may arise from (a) the selection of AOGCM; (b) the choice of carbon emission scenarios; (c) the choice of downscaling models (DSMs); (d) the selection of hydrological model and model parameters; and (e) the internal variability of the climate system. According to Prudhomme and Davies (2008), selection of AOGCMs creates more uncertainty in the downscaling process compared to the choice of emission scenarios or model parameterization. However, its also found that downscaling methods might be a significant source of uncertainty in hydrologic projections compared to the choice of climate models and emission scenarios that are a much less significant source of uncertainty (Bürger, Sobie, Cannon, Werner, & Murdock, 2012; Mandal, Breach, & Simonovic, 2016a). All the studies mentioned above they investigated only changes in climatic variables, for example, temperature or precipitation (Pr). Najafi, Moradkhani, and Jung (2011) conducted a study to compare uncertainties in predicted future flow stemming from different global climate models (GCMs), emission scenarios, and hydrological models. They considered eight GCMs, two emission scenarios from CMIP3 (Coupled Model Intercomparison Project 3) and four hydrologic models. The Tualatin river basin, Oregan, USA, was used as a study area. The study concludes that uncertainty in streamflow due to the GCMs structure is higher than the uncertainty due to the choice of the hydrologic model. However, Najafi et al. (2011) also suggested that hydrologic model selection is important when assessing hydrologic impacts under changing climate condition. The structural difference in hydrological models and uncertainties in parameter estimation can affect the spatial and temporal distribution of runoff. Recently, Surfleet and Tullos (2013) have conducted another study to explore uncertainties in predicted hydrologic response due to the choices of GCMs and a hydrological model. They selected the Santiam River basin in Oregon, USA, for case study purpose and found that GCM structure and parameterization contribute more to the uncertainties in predicted flow, compared to the contribution of hydrologic models. However, limited literature is available in Canada, which investigates all sources of uncertainty in streamflow projections under climate change. Schnorbus, Bennett, Werner, and Berland (2011) assessed the hydrologic impacts of climate change in three different watersheds (Peace, Campbell, and Columbia River) of British Columbia (BC), Canada. This investigation is conducted using a suite of eight GCMs with three emission scenarios. Climate variables from GCMs were downscaled using Bias Corrected Spatial Disaggregation method. This assessment concludes that GCMs are indeed a significant source of uncertainty when only a single DSM is used. Another study has been conducted by Das and Simonovic (2012) to assess uncertainty due to climate change in extreme flood flows for the Upper Thames River Basin, Ontario, Canada. In this study, three carbon emission scenarios and six GCMs with a single weather generator based on the k-nearest neighbour (K-NN) used for downscaling the climate variables. This study also found that different GCMs introduce more uncertainty compared to others sources. Dibike and Coulibaly (2005) assessed impacts of climate change on streamflow in the Saguenay watershed, Quebec, Canada. They used two DSMs and two hydrological models for this study. The results of their work show that the variation in river flow due to the choice of DSM is more significant than the variation introduced by choice of hydrological model. However, they did not consider variation due to the choice of emission scenario and/or GCMs.

Previously, most of the climate change assessment studies conducted in Canada were based on a single downscaling method except Dibike and Coulibaly (2005) who compared two downscaling tools and two hydrologic models. The main objective of this paper is to characterize the primary sources of uncertainty in simulated streamflow under changing climate conditions. The case study area is Campbell River basin, BC, Canada. The Campbell River is a coastal watershed in the central part of Vancouver Island. It consists of three reservoirs: Upper Campbell, Lower Campbell, and John Hart. From this river catchment, 1,230 GWh (gigawatt hours) of electricity is generated, which is equal to 11% of Vancouver Island's annual energy demand (BC Hydro Generation Resource Management, 2012). Hence, the variation in inflow into Campbell River reservoirs may have very significant economic and environmental consequences.

The detailed objectives of this study include quantification of the magnitude and frequency of streamflow in Campbell River basin considering three main sources of uncertainty introduced by the selection of downscaling methods, GCMs, and GHGs emission scenarios. Four GCMs, three emission scenarios, and six DSMs are used for this purpose. The UBC Watershed model (UBCWM; Quick & Pipes, 1977) is used for hydrologic flow simulation. Several studies (Kay, Davies, Bell, & Jones, 2009; Najafi et al., 2011; Surfleet & Tullos, 2013) concluded that GCMs structure is a larger source of uncertainty compare to hydrologic models and due to the limited resource, we used a single hydrologic model (UBCWM) for this study.

The following section of the paper describes the study area and data used. Section 3 provides the assessment framework, including a brief introduction of the hydrological model. Section 4 shows the details of hydrologic model calibration and validation. Results and discussion are presented in Section 5. Summary and conclusions are provided in Section 6.

2 | STUDY AREA AND DATA USED

The case study area, Campbell River watershed, is situated on the west coast of Canada (Figure 1a). This river basin is located in a transition zone between drier east coast and the wet west coast of Vancouver Island. The river originates from the mountains of central Vancouver Island and drains into the Strait of Georgia after traveling 33 km (Figure 1c). Total drainage area of this watershed is approximately 1,856 km^2 (BC Hydro Generation Resource Management, 2012). Annual average Pr during the last 20 years (1994 to 2013) in the catchment is 2,960 mm. The magnitude of Pr is high in the upstream section of the basin compared to downstream (Figure 1b). As the river originates from the west-facing mountains, orographic lifting of warm moist air from the Pacific Ocean causes heavy Pr in the upstream part

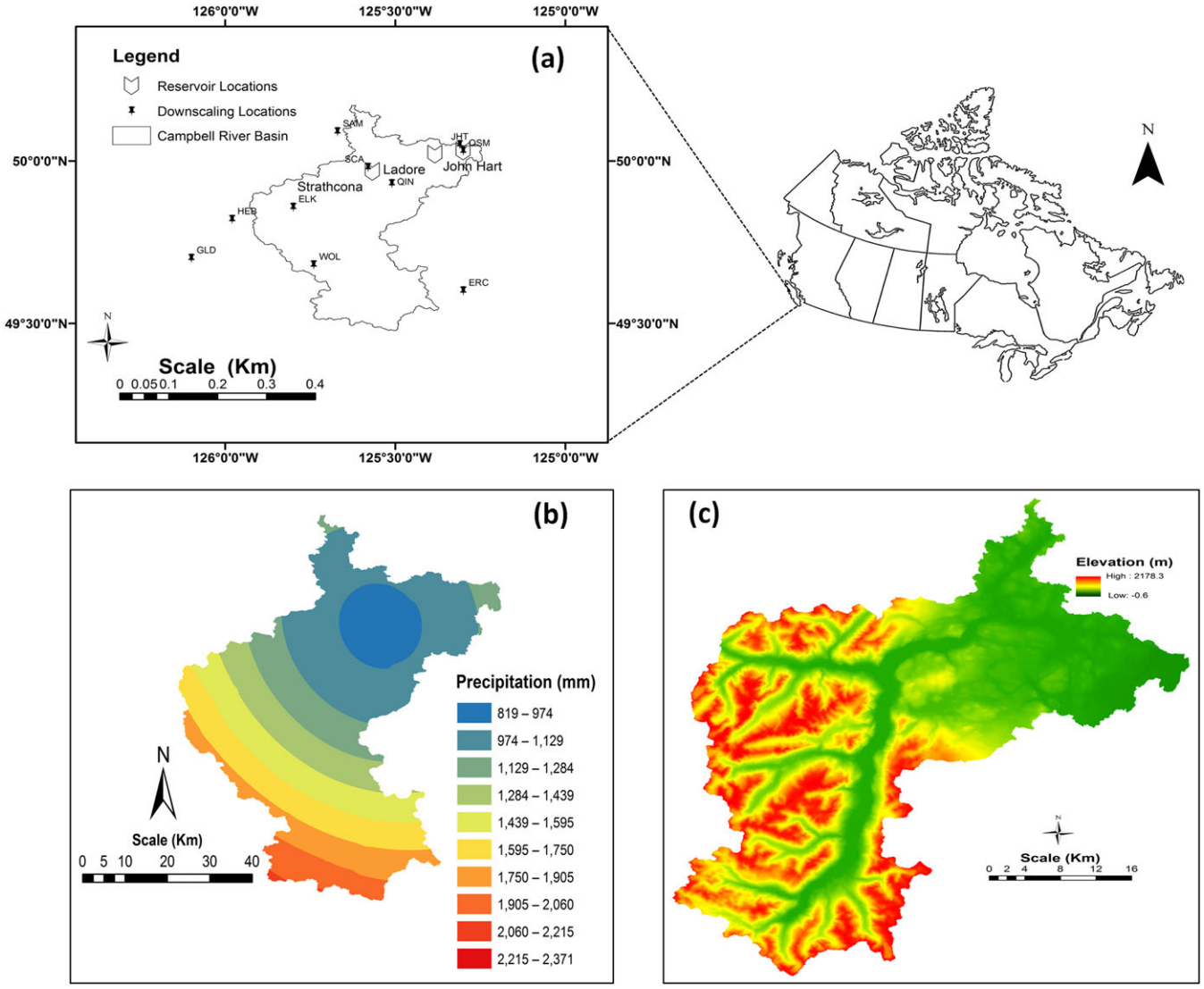

FIGURE 1 (a) Campbell River basin, British Columbia, Canada, with different downscaling locations and reservoirs location; (b) spatial representation of annual average precipitation (1994–2013); (c) digital elevation model of the Campbell River basin

of the basin. Campbell River includes three dams, Strathcona, Ladore, and John Hart (Figure 1a). Strathcona dam is located in the upstream section of the river, where other two are in the downstream section. Three reservoirs created by the dams are Upper Campbell Lake reservoir, Lower Campbell Lake reservoir, and John Hart Lake reservoir. The UBCWM hydrologic model simulates inflow into the Upper Campbell Lake reservoir, and the inflow into other two reservoirs is regulated by release from the Strathcona dam. The focus of this study is to assess the inflow variations into the Strathcona dam due to climate change. UBCWM is calibrated for the area upstream of Strathcona dam (1,176 km^2) excluding the Heber and Crest Diversions.

Daily time series of climate variables (e.g., Pr, maximum temperature [Tmax] and minimum temperature [Tmin]) are required for simulating flow using UBCWM. For two of downscaling methods, bias-corrected spatial disaggregation (BCSD) and bias correction constructed analogues with quantile mapping reordering (BCCAQ), climate variables (Pr, Tmax, and Tmin) are extracted from the Pacific Climate Impacts Consortium database (Pacific Climate Impacts Consortium U of V, 2014). For K-NN CAD v4 (K-NN weather generator) and maximum entropy bootstrap [MEB] weather generator, climate variables (Pr, Tmax, and Tmin) are obtained from Coupled Model Intercomparison Project 5 (CMIP5) database (IPCC, 2013). In addition to these variables, mean sea level pressure (mslp), specific humidity (hus) at 500 hPa, zonal (u-wind), and meridional (v-wind) wind are extracted from the CMIP5 repository for beta regression (BR) and kernel regression (KR) downscaling methods following Mandal, Srivastav, and Simonovic (2016b). All the climate variables extracted for the corresponding GCMs shown in Table 1. For the hydrologic model validation, historical daily inflow data (1984 to 2013) for the Strathcona dam has been obtained from the British Columbia Hydro (BC Hydro) repository.

3 | METHODOLOGY

A generalized framework for climate change impact assessment process is provided in Figure 2a. At first, climate models corresponding to different future emission scenarios (representative concentration pathways [RCPs]) are selected from a pool of climate models provided

TABLE 1 The GCMs used in the study

GCM model	GCM resolution (Lon. vs. Lat.)	Centre name
CanESM2	2.8 × 2.8	Canadian Centre For Climate Modeling And Analysis
CCSM4	1.25 × 0.94	National Center Of Atmospheric Research, USA
CSIRO-Mk3-6-0	1.8 × 1.8	Australian Commonwealth Scientific and Industrial Research Organization in collaboration with the Queensland Climate Change Centre of Excellence
GFDL-ESM2G	2.5 × 2.0	National Oceanic and Atmospheric Administration's Geophysical Fluid Dynamic Laboratory, USA

Note. GCMs = global climate models.

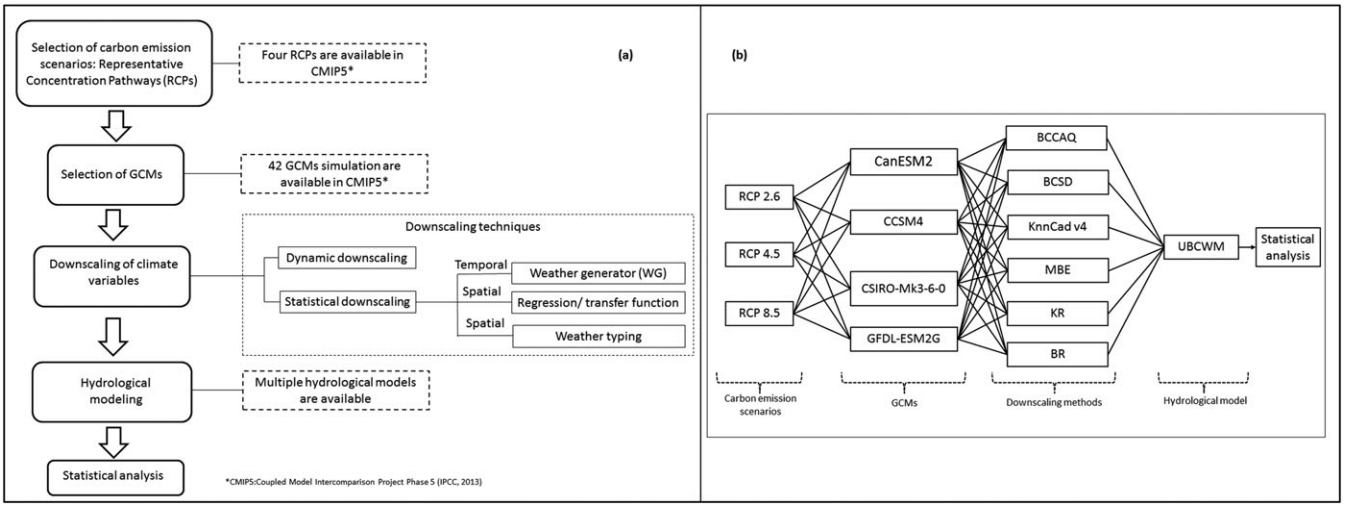

FIGURE 2 (a) Generalized framework of future streamflow generation under changing climate condition; (b) framework presenting the assessment process followed in this study. BCCAQ = bias correction constructed analogues with quantile mapping reordering; BR = beta regression; BSCD = bias-corrected spatial disaggregation; KR = Kernel regression; RCP = representative concentration pathway; UBCWM = UBC watershed model

in IPCC (2013). For this assessment of inflow uncertainty under changing climatic conditions, four GCMs are selected, and their details are given in Table 1. GCMs are selected based on the data availability for the implementation of downscaling methods (described below) used in this study. Four emission scenarios (RCP 2.6, RCP 4.5, RCP 6.0, and RCP 8.5) are suggested for use by the Fifth Assessment Report of Intergovernmental Panel on Climate Change IPCC; IPCC, 2013). RCP 2.6 is introduced as a lower GHGs emission scenario, RCP 4.5 and RCP 6.0 represent the intermediate GHGs emission scenarios, and RCP 8.5 describes the maximum and unabated GHGs emission conditions. For simulating future hydrologic flow, RCP 2.6, RCP 4.5, and RCP 8.5 are used in this study. RCP 4.5 is developed based on the assumption that GHGs emissions will be stabilized by mid-century and decrease after that where RCP 6.0 assumes that GHGs concentration will increase gradually and stabilize shortly after 2100 (van Vuuren et al., 2011). As the time frame of the study is up to 2100, RCP 4.5 is selected over RCP 6.0. Coarsely gridded GCMs data are required to downscale before it can be used for hydrologic analysis on a catchment scale. Six downscaling methods are used in this study: (a) BCSD (Bürger et al., 2012); (b) BCCAQ (Werner & Cannon, 2015); (c) delta change method coupled with a nonparametric K-NN weather generator (K-NN CAD v4; King, Mcleod, & Simonovic, 2015); (d) delta change method coupled with MEB weather generator (Srivastav & Simonovic, 2014); (e) nonparametric statistical DSM based on the KR (Kannan & Ghosh, 2013); and (f) BR-based statistical DSM (BR; Mandal et al., 2016b). A brief description of these downscaling processes is given in Appendix A.

Climate variables are obtained from four GCMs (Table 1) of CMIP5 for selected emission scenarios (IPCC, 2013). These variables are downscaled using different downscaling methods listed above. Downscaled GCM output is used as an input into a hydrological model to generate future flow series for the study area. Based on geospatial extents of a study, a distributed, semidistributed or lumped hydrologic models can be used for future flow generation. Hence, a continuous semidistributed hydrologic model (UBCWM) is used for this study. The framework of this assessment work is shown in Figure 2b. The details of the methodology followed are given below:

Step I: For downscaling purpose, climate variables (Pr, Tmax, Tmin, mslp, hus at 500 hPa, u-wind, and v-wind) are extracted from the CMIP5 repository. As GCM outputs have a different spatial resolution, all the climate data variables are spatially interpolated before downscaling to 10 different locations (Table 2) within the basin using inverse distance weighting (IDW) technique (Srivastav, Schardong, & Simonovic, 2014). According to this technique, data for a particular station is inversely proportional to the square of the distance between the station and the nearest grid data point. The weight associated with four nearest grid points to a particular

TABLE 2 Downscaling locations in the Campbell River basin, British Columbia, Canada

Station	Elevation (m)	Latitude (°N)	Longitude (°W)
Elk R ab Campbell Lk	270	49.85	125.8
Eric Creek	280	49.6	125.3
Gold R below Ucona R	10	49.7	126.1
Heber River near Gold River	215	49.82	125.98
John Hart Substation	15	50.05	125.31
Quinsam R at Argonaut Br	280	49.93	125.51
Quinsam R nr Campbell R	15	50.03	125.3
Salmon R ab Campbell Div	215	50.09	125.67
Strathcona Dam	249	49.98	125.58
Wolf River Upper	1490	49.68	125.74

station (v_i) can be calculated using Equation 1. Equation 2 is used for calculating the sum of the weighted average of climate variable for the station v_i.

$$W_j = \frac{\frac{1}{d_j^2}}{\frac{1}{d_1^2}+\frac{1}{d_2^2}+\frac{1}{d_3^2}+\frac{1}{d_4^2}} \quad (1)$$

$$v_i(t) = \sum_{j=1}^{4} W_j \times v_j(t) \quad (2)$$

where d_1, d_2, d_3, and d_4 are the distances of the station (v_i) from the four nearest grid points; v_j is climate variable value from the grid points; and $v_i(t)$ is the sum of weighted average for a particular time.

Step II: Using IDW, climate variables (Pr, Tmax, Tmin, mslp, hus at 500 hPa, u-wind, and v-wind) are interpolated for the near future period (2036 to 2065) and the far future period (2066–2095). These climate variables are used as input to downscaling. Four downscaling methods are used, including K-NN CAD v4, KR, BR, and MEB.

Step III: For BCCAQ and BCSD, gridded downscaled climate variables (Pr, Tmax, and Tmin) are obtained from Pacific Climate Impacts Consortium database. IDW is used to convert the gridded data into stations data.

Step IV: Climate data derived from the downscaling methods is spatially interpolated to be used by the UBCWM following Das and Simonovic (2012). The IDW method is used for patial interpolation (US Army Corps of Engineers, 2000).

Step V: The interpolated climate, variables (Pr, Tmax, and Tmin) are used by the calibrated UBCWM to simulate daily streamflow data for the two future time periods.

Step VI: At the end, statistical analysis has been performed to compare the simulated streamflow datasets with the observed data set. Python 3.2 is used for statistical analysis. For flow frequency analysis, we combined R "ismev" package (Heffernan, 2016) with Python.

In this study, the UBCWM is used to simulate streamflow in the Campbell River basin. This is a continuous hydrological model and only need Pr, Tmax, and Tmin to simulate flow. As the UBCWM was designed from minimum meteorological parameters, it is very useful in the mountainous watershed, for example, Campbell River watershed where meteorological and flows data are often spare (Micovic & Quick, 2009). Because the hydrologic response of a mountainous watershed depends on elevation, UBCWM adapted the "area-elevation band" concept. This concept includes orographic gradients of temperature and Pr that are assumed as dominate gradients of hydrological behavior in the mountainous catchment and act similarly for each storm. The UBCWM not only estimates streamflow in a catchment but also provides information about groundwater storage, soil moisture, surface and subsurface components of runoff, energy available for snowmelt, snowpack water equivalent, the area of snow cover, evapotranspiration, and interception losses (Quick & Pipes, 1977). The UBCWM integrates multiple meteorological submodels as described in (Micovic and Quick, 1999). The following sections provide information about hydrological model calibration and validation.

4 | HYDROLOGIC MODELLING

The hydrologic model UBCWM is calibrated by BC Hydro for Campbell river system and used in this study. UBCWM is available as a hydrological modeling framework under the name "Raven" (Craig & Snowdon, 2010). Raven considers a catchment as the integration of multiple subbasins where a number of noncontiguous and contiguous hydrological response units (HRUs) are assembled. Each HRU setup is based on a single combination of vegetation cover, terrain type, and land use or land type. Also, each HRU has a defined soil profile and stratified aquifer. Raven has a large number of user-customized subroutines, which can be used to develop a number of existing hydrologic models. UBCWM is emulated successfully in Raven by BC Hydro.

For this assessment purpose, the model is validated using observed data. Due to an inadequate amount of historical observed climate data, daily Pr, Tmax, and Tmin have been extracted from ANUSPLIN data set (0.1° latitude × 0.1° longitude), Environment Canada (Hutchinson & Xu, 2013). These data sets are extracted for a 20-year time period (1984 to 2013). ANUSPLIN data set is generated using "thin-plate smoothing spline" algorithm and broadly used in climate studies (Irwin, Srivastav, Simonovic, & Burn, 2016; Mandal et al., 2016b among others). As the ANUSPLIN data set has a different spatial resolution from GCMs, all the variables are spatially

interpolated using IDW to downscaling locations (Table 2) and used as input to the UBCWM. Multiple statistical indices, Nash–Sutcliffe efficiency (*NSE*) index, Pearson correlation coefficient (R^2), root mean square error (RSME), and relative bias are used to compare UBCWM simulated flow with the observed historical flow (1984 to 2013; Table 3) at different temporal scales. NSE index is a goodness-of-fit index, which is used to compare model simulated data with observed data. For accurate model prediction NSE should be 0. However, in this study, the value of NSE is high for all four temporal scales. For total annual flow, the NSE reaches 0.6, which is not acceptable. Dimensionless statistical index, for example, R^2 plays an important role in the assessment of both the hydrologic and statistical significance during a hydrologic model validation (McCuen, 2016). For example, if R^2 between predicted and measured values is high, that means the model outputs have quite similar pattern with measured values. R^2 varies between 0 to 1. High R^2 indicates a good correlation between observed and simulated data, which is desired. The results are showing R^2 values between 0.83 to 0.89 for different temporal scales. These values can be improved. RSME is a dimensioned statistical index, and low RSME is desired in hydrologic model validation. However, the results obtained in this study show a very high value of RSME, 6540.6 for total annual flow, which is not acceptable. Relative bias is used for comparing different data sets. Relative bias lower than 5% is usually recommended as the threshold value in hydrologic model validation (McCuen, 2016). However, the results obtained in this study show relative bias higher than 5%, which is again not satisfactory. Figure 3(a-d) presents time series comparison of simulated and observed flow at different temporal scales (daily, monthly, quarterly, and yearly). It shows that the UBCWM often fails to capture the extreme flow events. Figure 3(e-g), represents the Q-Q plot between model generated and historical daily, monthly, and quarterly flows, respectively. The Q-Q plots also show that for higher quantiles, simulated flow is not matching the observed data. However, if we review Figure 3(d) after 2010, the simulated streamflow matches with observed streamflow very well.

BC Hydro (BC Hydro Generation Resource Management, 2012) reported that the Herber dam used to release water into the Campbell River system until 2012 when it was decommissioned. The Herber river is located approximately 70 km west of the city of Campbell river. It naturally flows southwest for approximately 14 km before joining the Elk river, which later joins Strathcona reservoir. During this 14-km stretch, the Herber river connects Crest lake, Mud lake, and Upper and Lower Drum lakes before joining the Elk river. The Herber river connects with Crest lake through a wood stave and diverts water, when available. The Herber diversion used to divert on average 1.1 m^3/s into Elk river where annual mean inflow to Strathcona reservoir is 77.5 m^3/s. Although the diverted flow from Herber diversion is much smaller than the inflow into Strathcona reservoir, the total annual amount of 35 Mm^3/year represents a significant contribution to the Strathcona reservoir volume. The Herber diversion has been decommissioned in 2010 (BC Hydro Generation Resource Management, 2012). The hydrologic model (UBCWM) was calibrated in 2014 by BC Hydro. Therefore, UBCWM does not consider additional flow from the Herber dam before 2010 and that is the possible explanation for unsatisfactory validation results. For further investigation, the new validation period has been selected, 2012–2013, for daily and monthly streamflow analyses. For yearly flow validation, we considered a 3-year time span (2010 to 2013). The validation results for a new period are shown in Table 4. Due to inadequate data set after 2013, we selected 3 years (2010–2013) for new validation period. There are studies (Asokan & Dutta, 2008; Refsgaard, 1997) conducted in the past using less than 5 years of data for hydrological model validation. For the new validation period (2010 to 2013), the NSE value is improved compared to the validation using 1984–2013 period. The NSE value for total annual flow is 0.08. An improvement is also observed for other three indexes. Relative bias is lower than 5% for all four temporal scales. Simulated daily, monthly, quarterly, and yearly streamflow for new validation period are shown in Figures 4(a-d), respectively. These plots confirm that the UBCWM generated flow is quite similar to the observed flow. Figure 4(f) shows a Q-Q plot between model generated and historical flows. It also certifies that the UBCWM model generated streamflow matches historical flow. Therefore, from the validation analyses, it can be concluded that the UBCWM performs well in capturing historical flow.

5 | RESULTS AND DISCUSSION

Downscaled climate variables (Pr, Tmax, and Tmin) are used with the hydrologic model for future flow generation. The simulated flow is generated and analyzed for two future time periods (2036–2065 and 2066–2095). Figures 5–7 present cumulative distribution function (CDF) of simulated flow for different emission scenarios, GCMs and DSMs, respectively. The CDF is a useful tool for assessing the intensity of the occurrence of high/low flow in the catchment. It has been found that CDFs obtained from different emission scenarios are quite similar (Figure 5). A similar pattern can be found in Figures 6 and 7. However, RCP 4.5 and RCP 8.5 show the high intensity of flow compared to historical flow in the near future (2036–2065; Figure 5c and 5e). In far future (2066–2095), a high intensity flow is found for RCP 2.6 and RCP 8.5 (Figure 5b and 5f). Another observation is that flow intensity in higher quantiles is subject to higher uncertainty for different RCPs and GCMs (Figures 5 and 6). However, Figure 7 shows that in higher quantile CDFs are less flattered compare to Figures 5 and 6. Results

TABLE 3 Hydrological model performance statistics (1984–2013) in the Campbell River basin, British Columbia, Canada

Time period	Nash–Sutcliffe efficiency (*NSE*)	Pearson correlation coefficient (R^2)	Root mean square error (RSME)	Relative bias (%*Bias*)
Total daily flow	0.35	0.83	46.78	−13.69
Total monthly flow	0.39	0.88	296.33	−13.72
Total quarterly flow	0.36	0.89	563.20	−13.72
Total annual flow	0.60	0.85	6540.60	−11.32

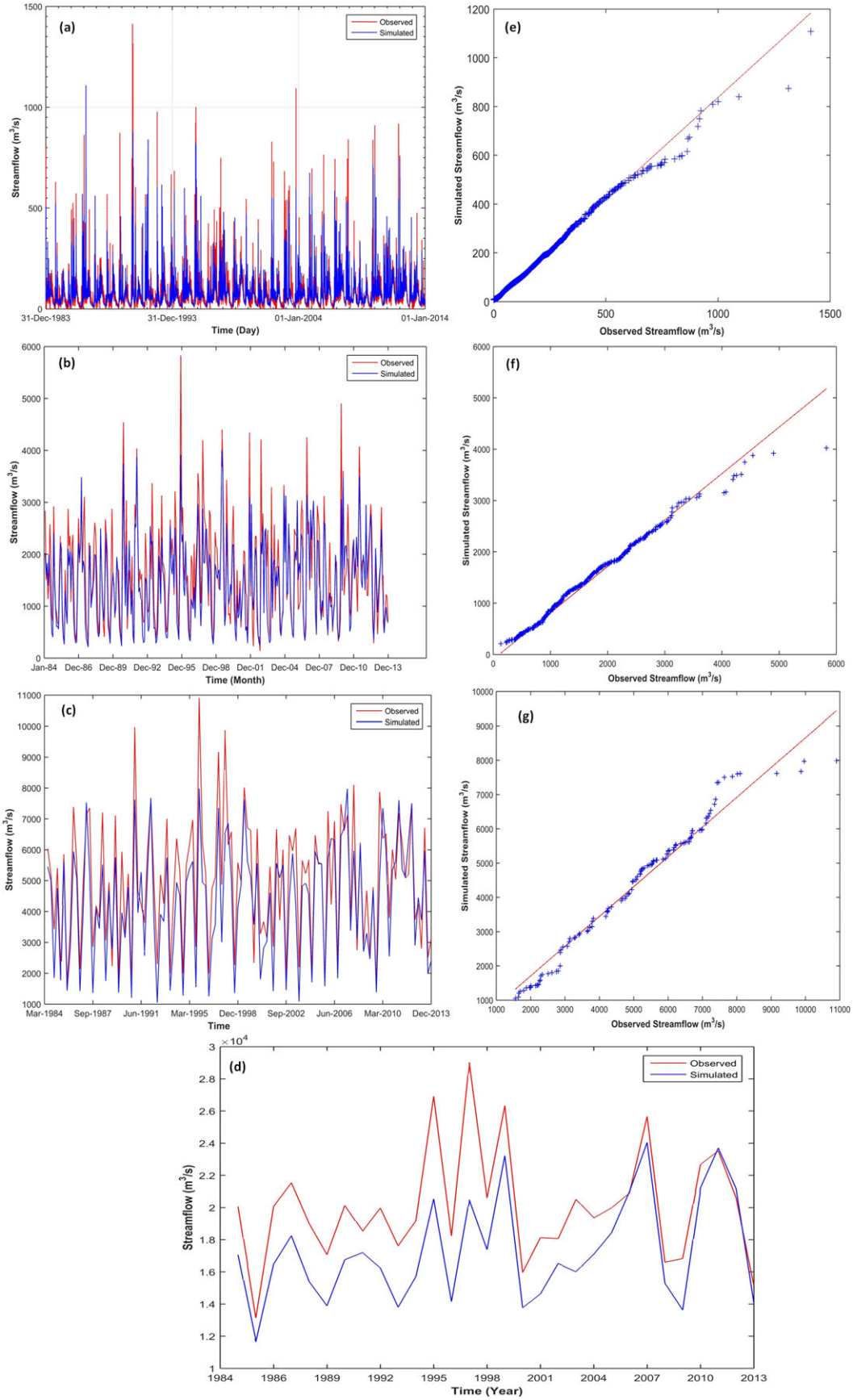

FIGURE 3 (a-d) Daily, monthly, quarterly, and yearly simulated and observed total inflow into the Strathcona reservoir, British Columbia, Canada, respectively, (1984–2013); (e-g) daily, monthly, and quarterly Q-Q plot of simulated and observed total inflow into the Strathcona reservoir (1984–2013), respectively

TABLE 4 Hydrological model performance statistics for (2012–2013) in the Campbell River basin, British Columbia, Canada

Period	Nash–Sutcliffe efficiency (*NSE*)	Pearson correlation coefficient (R^2)	Root mean square error (RSME)	Relative bias (%*Bias*)
Total daily flow	0.27	0.87	30.61	−2.28
Total monthly flow	0.18	0.91	210.67	−1.40
Total quarterly flow	0.15	0.92	421.56	−1.40
Total annual flow (2010–2013)	0.08	0.97	952.51	−2.16

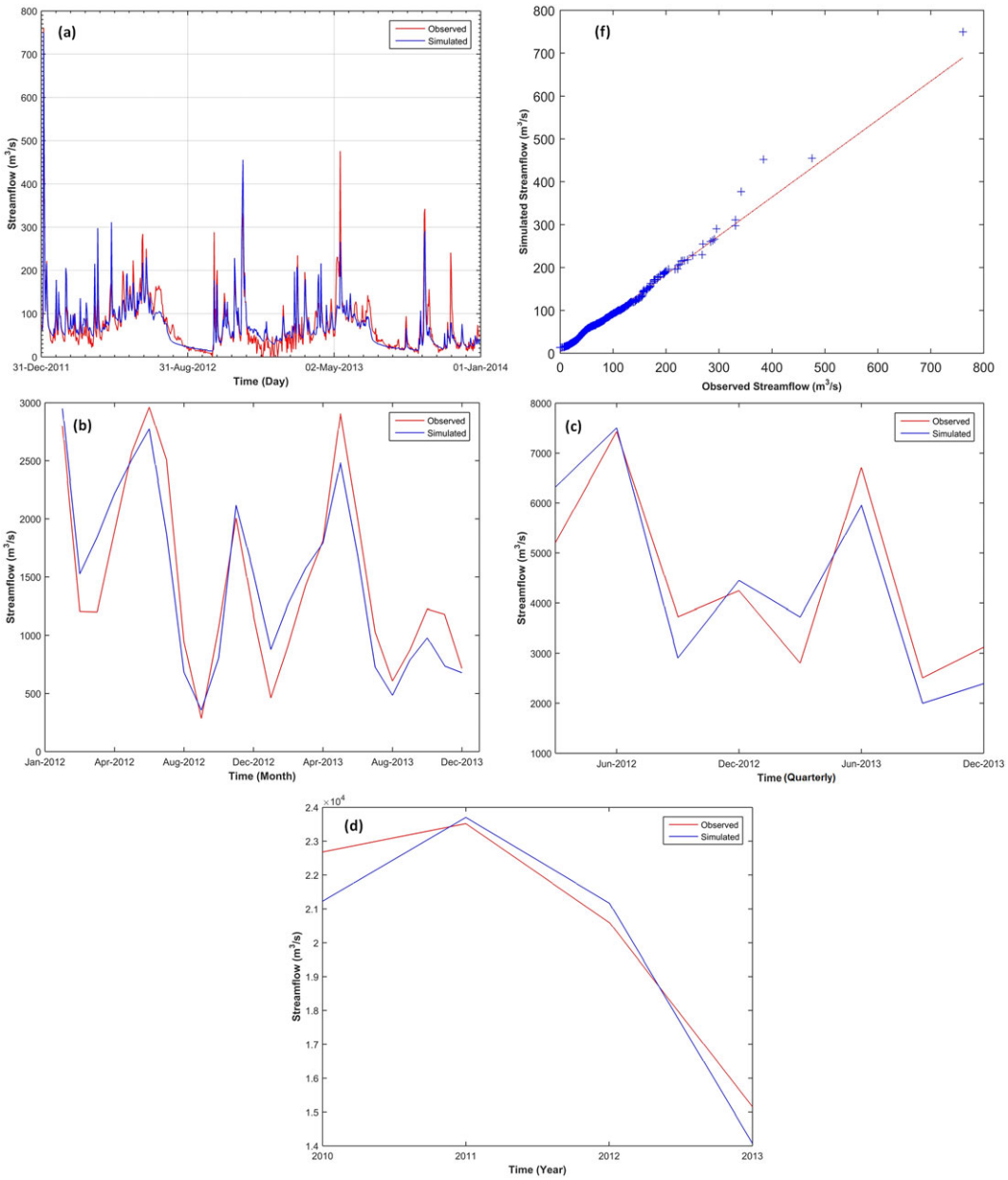

FIGURE 4 (a-d) Daily (2012–2013), monthly (2012–2013), quarterly (2012–2013), and yearly (2010–2013) simulated and observed total inflow of the Strathcona reservoir respectively; (f) daily Q-Q plot of simulated and observed total inflow of the Strathcona reservoir (2012–2013)

in Figures 5 and 6 are generated for fixed choice of DSMs (BCSD, BCAAQ, BR, KR, K-NN CAD v4, and MEB), wherein Figure 7, the resulting CDFs are obtained for different DSMs. Different DSMs are developed using different statistical methods and assumption, and therefore, the downscaled values may show variation in flow intensity. For further investigation, comparison of a single combination of RCP, GCM, and DSM is included in Figure 8. Results in Figure 8 confirm that variations in streamflow due to the choice of DSMs are higher compared to the variations due to the selection of RCPs or GCMs.

Average historical and future seasonal flow statistics for different RCPs, GCMs, and DSMs are shown in Tables 5–7, respectively. Table 5 indicates that mean winter flow will increase, with estimated range between 13% to 19% in the near future (2036–2065) and 15% to 29% in the far future (2066–2095) for different emission scenarios.

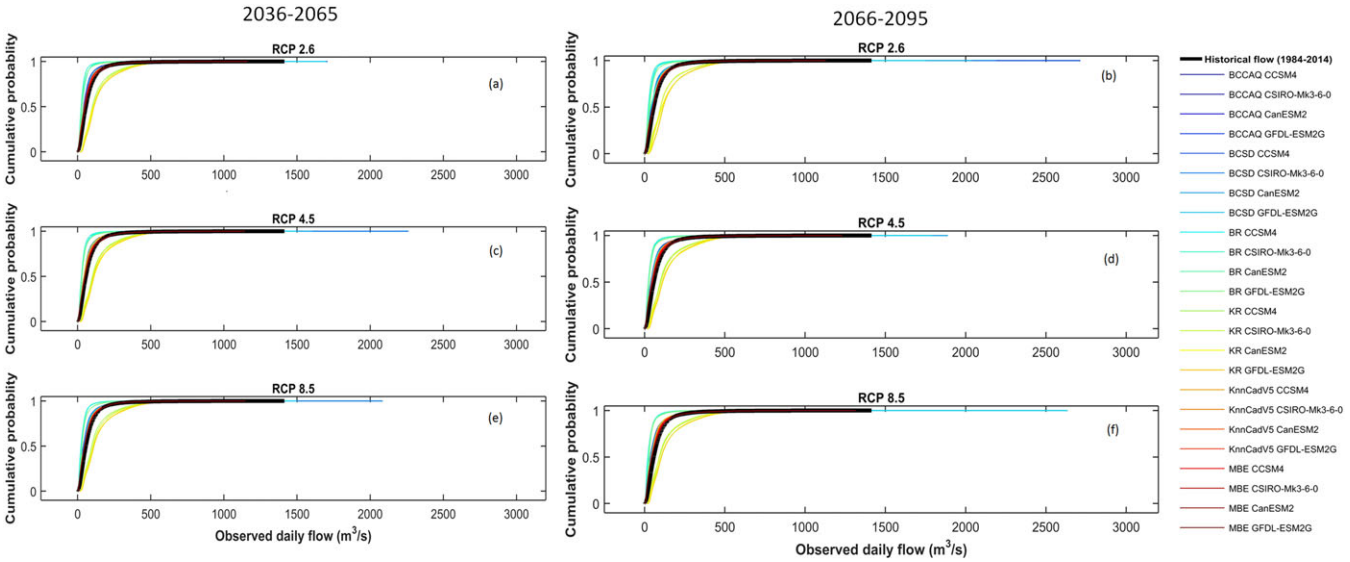

FIGURE 5 Cumulative probability distribution of simulated (2036–2065 and 2066–2095) and historical (1984–2013) daily streamflow into the Strathcona reservoir, BC, Canada for different emission scenarios. BCCAQ = bias correction constructed analogues with quantile mapping reordering; BCSD = bias-corrected spatial disaggregation; BR = beta regression; RCP = representative concentration pathway

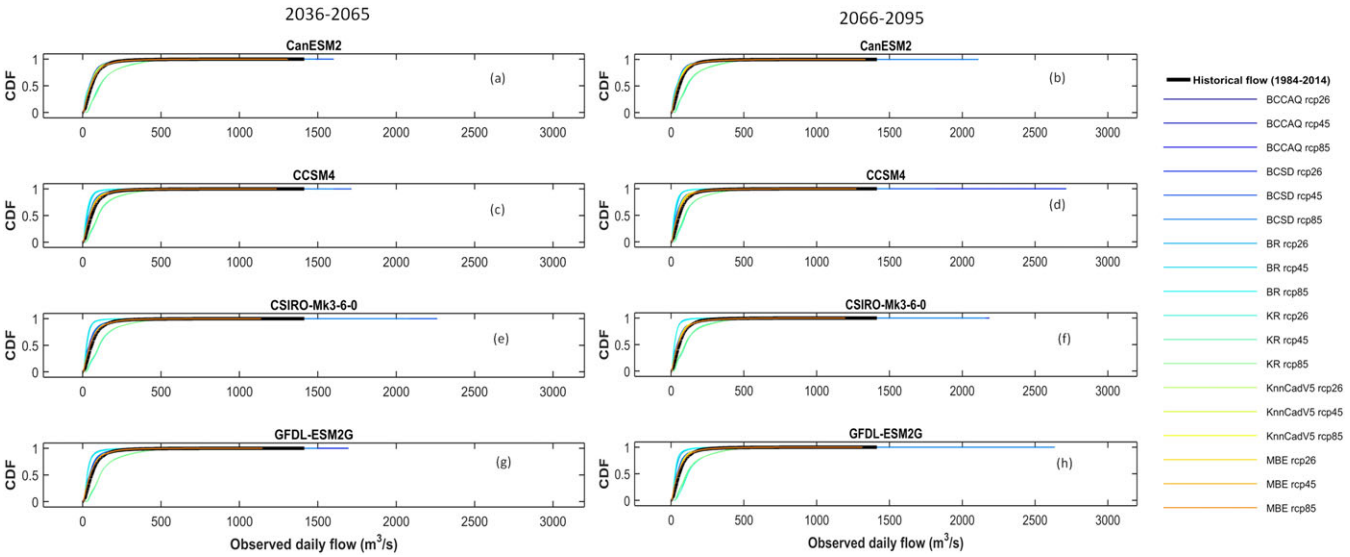

FIGURE 6 Cumulative probability distribution (CDF) of simulated (2036–2065 and 2066–2095) and historical (1984–2013) daily streamflow into the Strathcona reservoir, BC, Canada for different global climate models

However, summer mean streamflow will decrease by at least 51% in the near future and 66% in the far future (Table 5). A similar kind of trend is found in Tables 6 and 7.

The results indicated that the winter flow will increase where other seasonal flow will decrease, in both future time periods (Tables 6 and 7). Summer flow will decrease from 49% to 57% in near future and 58% to 66% in the far future where winter flow will increase 5% to 23% and 13% to 32% in near and far future, respectively, for different GCMs (Table 6). Results indicate that the summer flow in the near future will be reduced up to a maximum of 69% compared to the historical flow where the highest decrease in the flow of 71% may be experienced in the far future (Table 7). Only the KR model provides different results (Table 7). To summarize, the summer flow in the Campbell River basin (BC, Canada) will be highly affected by the changing climate conditions. Spring flow will range from −9% to −19% and −12% to −52% for near and far future, respectively, except for KR model results. Streamflow during fall will decrease in the range from −7% to −23% and −2% to −49% for near and far future, respectively, except KR model results.

Figures 9–11 present box plots of projected mean monthly simulated streamflow with the historical flow. It is clearly visible that the mean monthly flow in Figures 9 and 10 is quite different when compared to the flows in Figure 11. In Figure 11, for summer months (May, June, and July), future flows for both time periods are less than historical summer mean flows. However, in Figure 11, variation in mean monthly flows is very less compared to Figures 9 and 10. These results also support the hypothesis that the choice of DSMs introduces a higher level of uncertainty in streamflow prediction compared to the

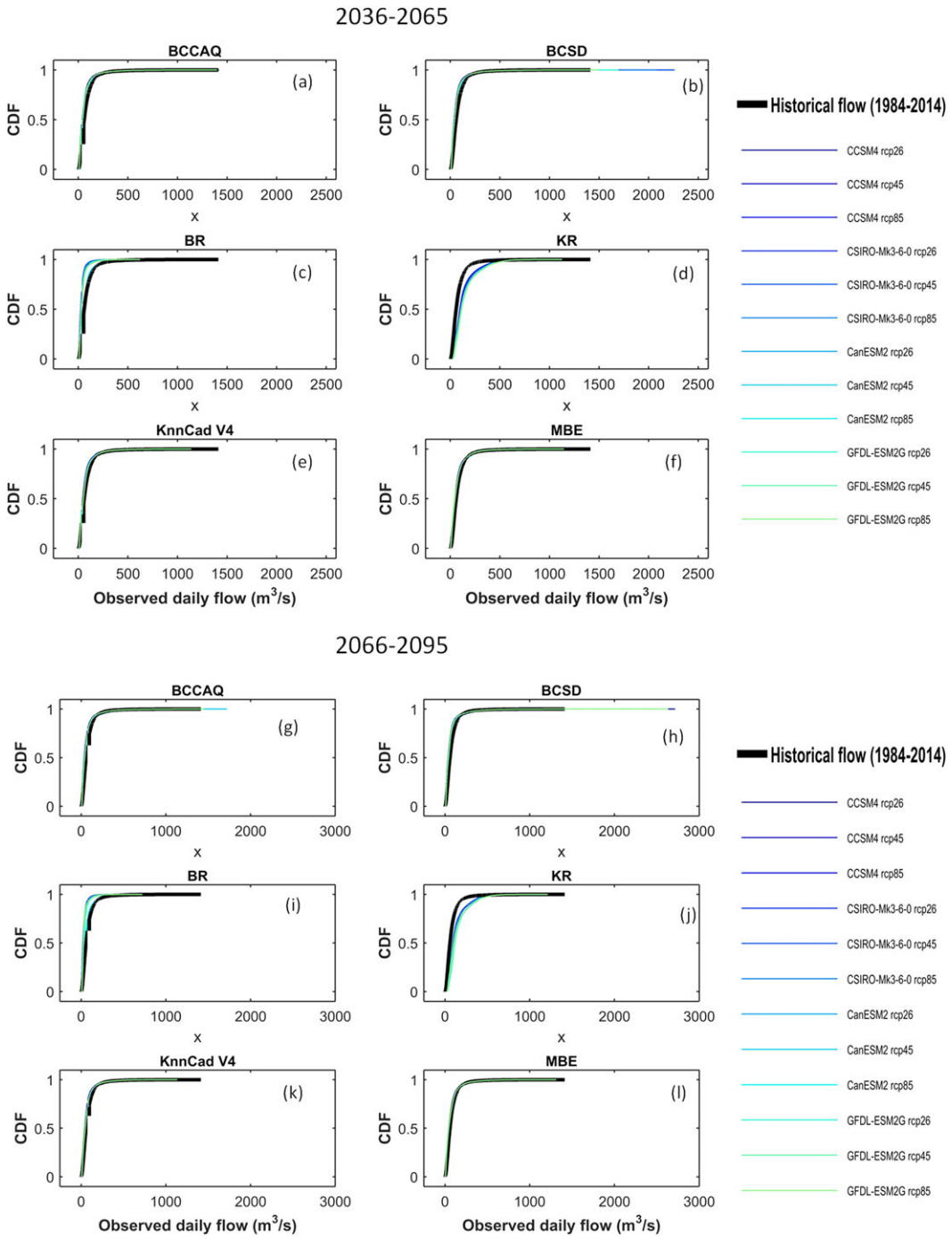

FIGURE 7 Cumulative probability distribution (CDF) of simulated (2036–2065 and 2066–2095) and historical (1984–2013) daily streamflow of the Strathcona dam, BC, Canada for different downscaling methods. BCAAQ: Bias correction constructed analogues with quantile mapping reordering; BCSD: Bias corrected spatial disaggregation; BR: Beta regression based statistical downscaling model; KR: Nonparametric statistical downscaling model based on the Kernel regression; KnnCAD v4: Delta change method coupled with a nonparametric K-nearest neighbor weather generator; MBE: Delta change method coupled with maximum entropy weather generator (MBE)

choice of RCPs and GCMs. In addition, the results in Figure 10 confirm that future summers will be drier and future winters will be wetter compared to the historical time period (1984–2013). Schnorbus et al. (2011) investigated hydrologic impacts of climate change in the Campbell River basin where they found that decreasing trend (−14% for A1B scenario) in future Pr (2041 to 2070) for June, July, and August and increasing trend (5% to 11%) in October through December. This study also found that monthly mean temperature would have a significant and strong signal of shifting to warmer temperature throughout the year and particularly higher for July, August, and September in future (2041 to 2070). Streamflow in the Campbell River is fed by a mix of rain and snowmelt. As the temperature is increasing, it has been predicted that snowfall will decrease throughout the fall and winter where rainfall will increase (Schnorbus et al., 2011) in this river basin. This leads to a conclusion that the streamflow in this river basin will be rainfall dominated compare to the hybrid mix (snow and rain). Due to projected higher temperature in mid-winter and early spring (Schnorbus et al., 2011), snow will melt faster than before, whereas

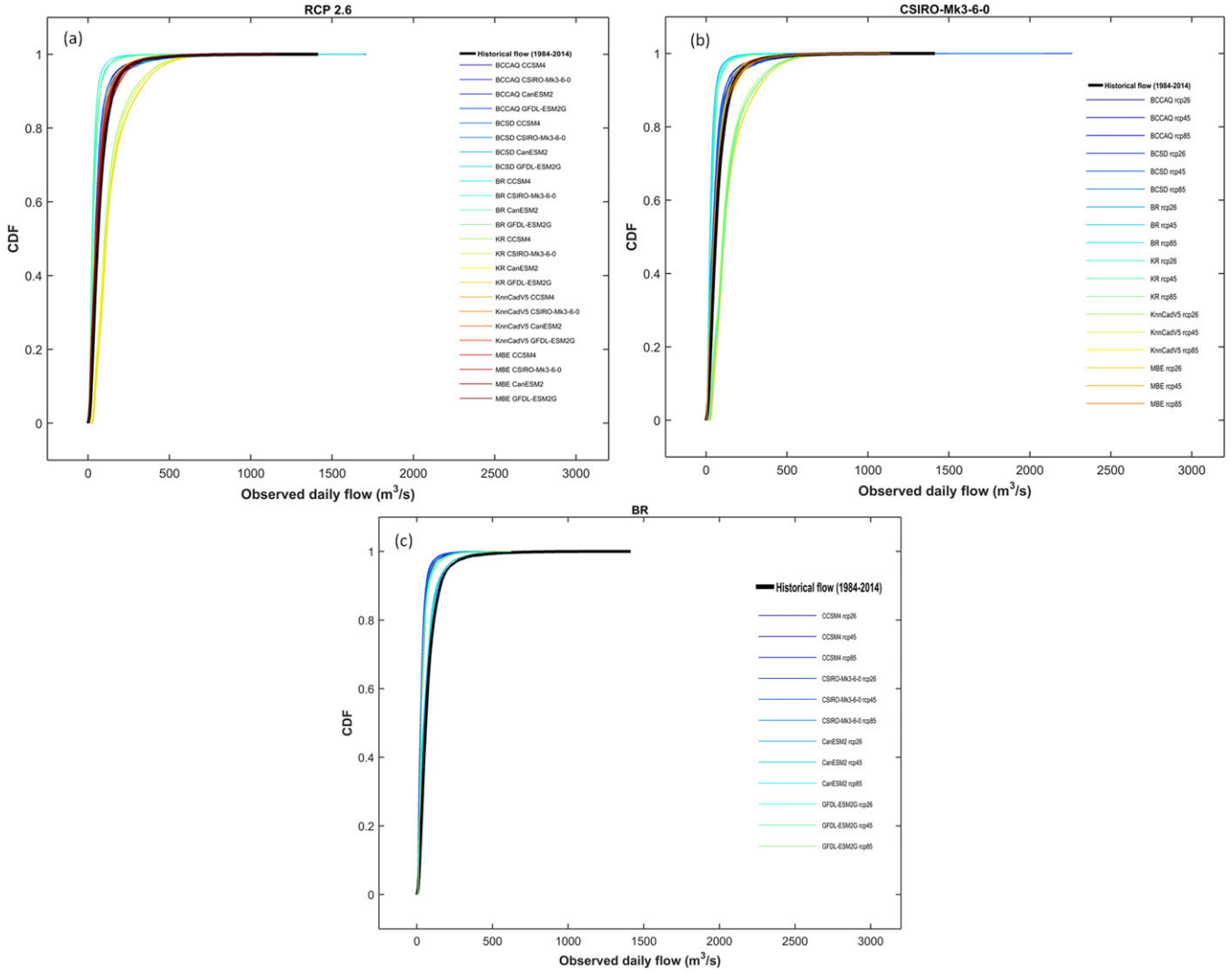

FIGURE 8 Cumulative probability distribution (CDF) of simulated (2036–2065) and historical (1984–2013) daily streamflow of the Strathcona dam, BC, Canada for (a) RCP 2.6; (b) CSIRO-Mk-3-6-0; and (c) beta regression (BR)-based statistical downscaling model

less snow will be available for melt because of significant reduction of historical spring freshet. This evidence is the possible reason behind the increasing flow in winter and less flow in summer (Figure 10). From this study, it can be concluded that the Campbell River basin will become a pluvial regime (rainfall dominated) in future from the hybrid nival–pluvial regime (snow influenced). Schnorbus et al. (2011) also provided similar conclusion in their study. The details about flow frequency analysis are given in the following section.

5.1 | Flow frequency analysis

The generalized extreme value (GEV) distribution is used for flow frequency analysis. GEV is an integration of continuous probability distributions that combines the Gumbel (EV1), Frechet, and Weibull distributions and is widely used in flow frequency analysis (Das, Millington, & Simonovic, 2013; Das & Simonovic, 2012; Fowler & Wilby, 2010). The GEV has three parameters, for example, location, shape, and scale. The shift in the distribution is described by the location parameter where the scale parameter describes the spread of the distribution and the shape parameter describes the skewness. If the shape parameter (k) = 0, GEV becomes Gumbel distribution, and when k < 0, it is transformed in Weibull distribution. If k > 0, then the GEV is converted into the Frechet distribution. CDF and probability distribution function of GEV are defined as follows (Hosking & Wallis, 1997):

$$F(x;\alpha,\kappa,\xi) = \exp\left\{-(y)^{-\frac{1}{\kappa}}\right\} \quad \text{when } y\rangle 0 \ \& \ \kappa \neq 0 \tag{3}$$

$$= \exp\left(-\exp\left(\frac{x-\xi}{\alpha}\right)\right) \quad \text{when } \kappa = 0 \tag{4}$$

$$f(x;\alpha,\kappa,\xi) = \alpha^{-1}[y]^{\left(-1-\frac{1}{\kappa}\right)}\exp\left(-y^{-\frac{1}{\kappa}}\right) \quad \text{when } \kappa \neq 0 \tag{5}$$

$$= \alpha^{-1}\exp\left[-\left(\frac{x-\xi}{\alpha}\right)\right]\exp\left\{-\exp\left[-\left(\frac{x-\xi}{\alpha}\right)\right]\right\} \quad \text{when } \kappa = 0, \tag{6}$$

where $y = \left[1+\kappa\left(\frac{x-\xi}{\alpha}\right)\right]$; ξ is the location parameter; $\alpha$is the scale parameter; and $\kappa$is the shape parameter.

The flow frequency analysis is conducted using ismev package in R-studio combined with python environment (Heffernan, 2016). The flow frequency curves are shown in Figure 12. The flow frequency

TABLE 5 Historical (1984–2013) and future mean seasonal flows (m^3/s) (5th, median—50th, and 95th percentile estimates) for different emission scenarios in Upper Campbell Lake reservoir, British Columbia, Canada

		2036–2065				2066–2095			
	Historical	5th	50th	95th	Change in median value (%)	5th	50th	95th	Change in median value (%)
RCP 2.6									
Winter	7602	4553	8591	15397	13	4586	8744	15233	15
Spring	7763	4202	6772	16726	−12	4115	6750	16459	−13
Summer	6661	1726	3254	7282	−51	1518	3393	6650	−49
Fall	6924	3245	5714	12990	−17	2729	5821	12853	−15
RCP 4.5									
Winter	7602	4758	9094	16221	19	4763	9306	16897	22
Spring	7763	4085	6681	15319	−13	3346	6568	14821	−15
Summer	6661	1745	3232	7110	−51	1608	2697	6062	−59
Fall	6924	3142	5895	13382	−14	3021	6260	13312	−9
RCP 8.5									
Winter	7602	4896	8884	16962	16	4663	9802	17312	29
Spring	7763	3925	6528	15558	−16	2922	6111	13857	−21
Summer	6661	1631	2694	6235	−59	1276	2265	5686	−66
Fall	6924	2645	5612	13342	−19	3341	5912	12930	−14

Note. RCP = RCP=representative concentration pathway.

TABLE 6 Historical (1984–2013) and future mean seasonal flows (m^3/s) (5th, median—50th, and 95th percentile estimates) for different GCMs in Upper Campbell Lake reservoir, British Columbia, Canada

		2036–2065				2066–2095			
	Historical	5th	50th	95th	Change in median value (%)	5th	50th	95th	Change in median value (%)
CCSM4									
Winter	7602	5324	7999	14413	5	5320	8620	15422	13
Spring	7762	3814	6229	15238	−19	3137	6436	14369	−17
Summer	6661	1455	3000	6441	−54	1241	2506	5924	−62
Fall	6923	2812	5302	13040	−23	2481	5498	12706	−20
CSIRO-Mk3-6-0									
Winter	7602	4186	9053	16274	19	4524	10023	16261	31
Spring	7762	3877	7021	15699	−9	3223	6567	14184	−15
Summer	6661	1802	3332	6103	−49	1473	2373	5440	−64
Fall	6923	2375	6371	12974	−7	2539	6727	12945	−2
CanESM2									
Winter	7602	8569	9368	16284	23	8446	10054	17810	32
Spring	7762	6272	6942	18321	−10	5168	6604	16728	−14
Summer	6661	1605	2855	7172	−57	1422	2242	6207	−66
Fall	6923	5294	5985	13105	−13	5165	6048	12729	−12
GFDL-ESM2G									
Winter	7602	4561	8925	16994	17	4357	9426	17082	24
Spring	7762	4682	6694	15561	−13	3621	6682	15175	−13
Summer	6661	1771	3358	7569	−49	1771	2771	7242	−58
Fall	6923	3883	5580	14911	−19	4025	5768	15531	−16

curve derived from the observed historical data is also shown in Figure 12. The results are presented for various return periods from 2 to 200 years. The figure summarizes the impact of choosing different GCMs and DSMs on the flows corresponding to different return periods. It is found that the uncertainty increases with the increase in the return period where CDFs become flattered. It is also found that in the far future, CDFs are flatter compared to the near future time period. The average percentage changes in flow magnitudes are shown in Table 8. The maximum average percentage changes of the 50-year flow magnitude between future climate (2036–2065 and 2065–

TABLE 7 Historical (1984–2013) and future mean seasonal flows (m^3/s) (5th, median—50th, and 95th percentile estimates) for different downscaling methods in Upper Campbell Lake reservoir, British Columbia, Canada

Downscaling method		Historical	5th	Median	95th	Change in median value (%)	5th	Median	95th	Change in median value (%)
BCCAQ	Winter	7602	8382	9493	10884	24	8846	10284	11313	35
	Spring	7762	5807	6260	6877	−19	5466	5878	6403	−24
	Summer	6661	1791	2019	2324	−69	1587	1886	2403	−71
	Fall	6923	5361	5935	7098	−14	5419	6094	7686	−11
BR	Winter	7602	6601	7479	12394	−1	4175	4927	10806	−35
	Spring	7762	6111	6782	8840	−12	2829	3651	5830	−52
	Summer	6661	3903	4251	4562	−36	1179	1530	2038	−77
	Fall	6923	4752	5850	8945	−15	2373	3523	5783	−49
KR	Winter	7602	9995	12077	13866	58	10426	12499	13846	64
	Spring	7762	11003	11756	14867	51	8810	10688	12997	37
	Summer	6661	1577	2813	4195	−57	3905	4893	6890	−26
	Fall	6923	8307	9138	11452	31	8289	8917	11578	28
BCSD	Winter	7602	8150	9170	9918	20	8627	9636	10918	26
	Spring	7762	6098	6358	7237	−18	5378	5830	6749	−25
	Summer	6661	1889	2156	2520	−67	1618	1879	2530	−71
	Fall	6923	4889	5602	6374	−19	5351	6075	6897	−12
KnnCADV4	Winter	7602	7218	8334	8942	9	7786	8502	9517	12
	Spring	7762	6663	7003	7553	−9	6304	6752	7412	−13
	Summer	6661	3601	4259	4960	−36	2423	3629	5121	−45
	Fall	6923	4946	5459	6450	−21	4864	5497	6353	−20
MBE	Winter	7602	7589	8257	9223	8	7858	8796	9998	15
	Spring	7762	6386	6942	7624	−10	6594	6818	7344	−12
	Summer	6661	4560	5243	5724	−21	3070	4488	6087	−32
	Fall	6923	5194	5846	6468	−15	5246	5911	6722	−14

Note. BCCAQ=bias correction constructed analogues with quantile mapping reordering; BCSD=bias-corrected spatial disaggregation; BR=beta regression; KR=Kernel regression.

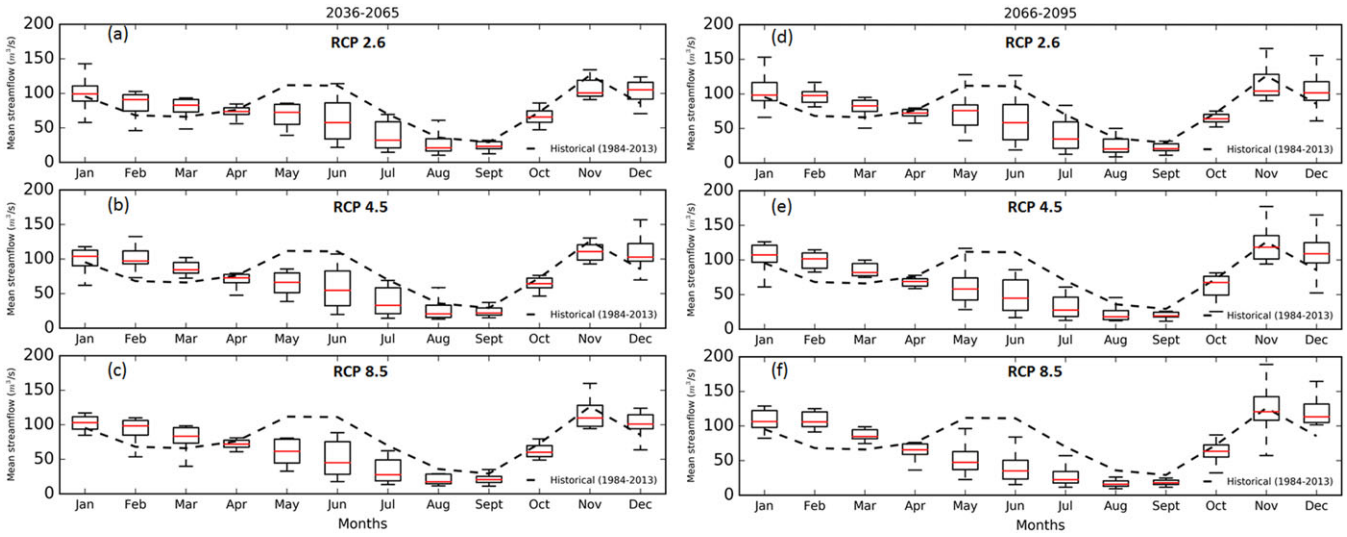

FIGURE 9 Boxplots showing projected mean monthly simulated streamflow for the near future (2036–2065) and the far future (2066–2095) with historical (1984–2013) observed flow into the Strathcona dam, BC, Canada for different emission scenarios. RCP=representative concentration pathway

2095), and the historical (1984–2013) are, respectively, −20.2% and −5.7%. In the near future, for RCP 8.5, a decreasing trend is observed with the increase in the return period. On the contrary, in the far future for RCP 8.5, an increasing trend is observed with the increase in the return period. RCP 8.5 considers maximum amount of GHGs emission in the atmosphere, which is approximately three times of today's carbon emission by the end of this century (van Vuuren et al., 2011). GHGs emissions have a positive correlation with atmospheric temperature (IPCC, 2013). Therefore, the Pr pattern can be changed significantly. This can be a possible reason for decreasing trend of flow magnitude for near future. Table 9 shows a comparison between historical and future flow return periods for different emission scenarios. For all emission scenarios, the return period of higher flow event will increase in both future time periods. For example, 1,250 m^3/s flow had a return period of 11 years, but it will change to 20 years (2036–2065) and 21 years (2066–2095) for RCP 2.6 emission scenarios (almost doubled). A similar trend could be found for other emission scenarios too.

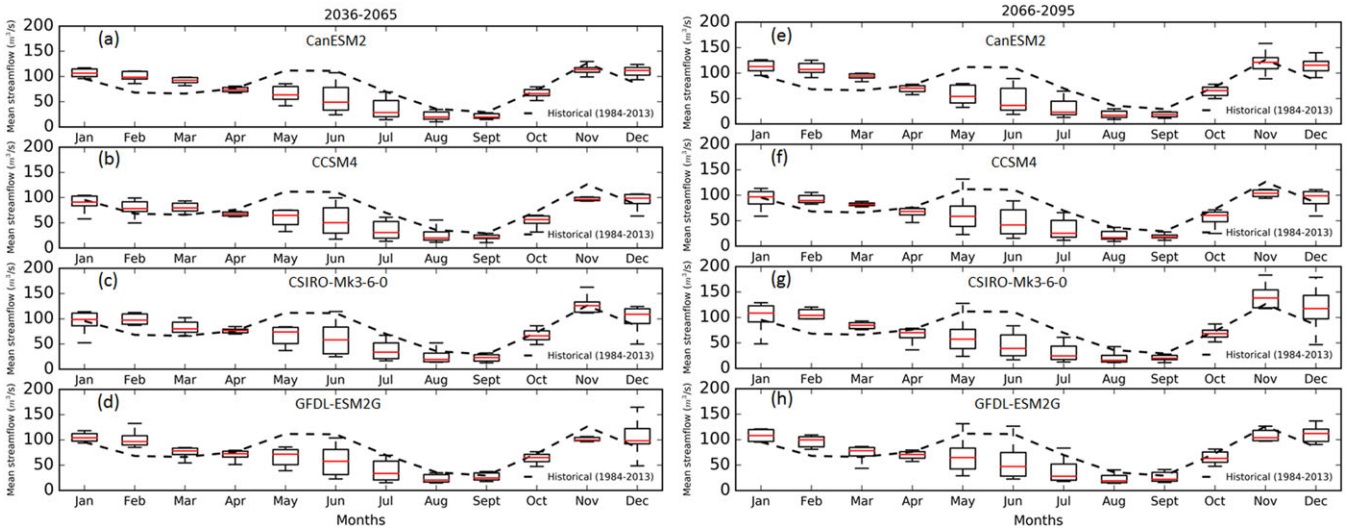

FIGURE 10 Boxplots showing projected mean monthly simulated streamflow for the near future (2036–2065) and the far future (2066–2095) with historical (1984–2013) observed flow into the Strathcona dam, BC, Canada for different global climate models

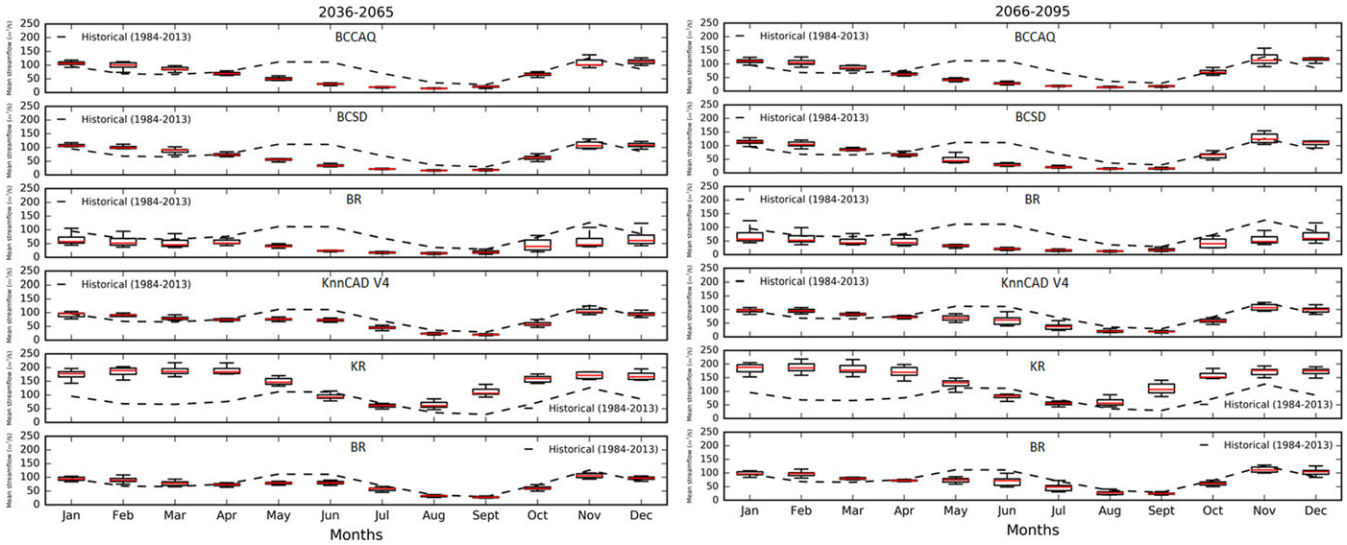

FIGURE 11 Boxplots showing projected mean monthly simulated streamflow for the near future (2036–2065) and the far future (2066–2095) with historical (1984–2013) observed flow into the Strathcona dam, BC, Canada for different downscaling models. BCCAQ = bias correction constructed analogues with quantile mapping reordering; BCSD = bias-corrected spatial disaggregation; BR = beta regression; KR = Kernel regression

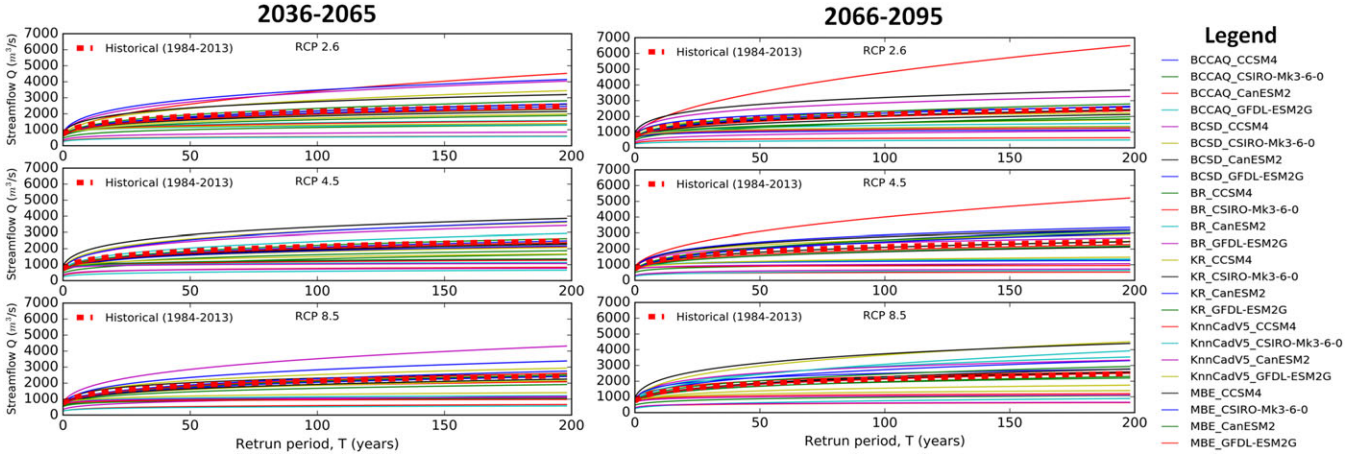

FIGURE 12 Simulated flow frequency results of the Strathcona dam, BC, Canada using GEV for different emission scenarios between two future time periods. BCCAQ = bias correction constructed analogues with quantile mapping reordering; BCSD = bias-corrected spatial disaggregation; BR = beta regression; KR = Kernel regression; RCP = representative concentration pathway

TABLE 8 Average percentage changes in streamflow magnitude between baseline period (1984–2013) and future time periods in Upper Campbell Lake reservoir, British Columbia, Canada

	2036–2065			2066–2095		
Return period (year)	RCP 2.6	RCP 4.5	RCP 8.5	RCP 2.6	RCP 4.5	RCP 8.5
5	−14.0	−13.2	−16.1	−13.8	−12.5	−6.6
10	−14.1	−14.4	−17.8	−15.0	−13.6	−6.8
50	−13.0	−16.1	−20.2	−16.0	−14.4	−5.7
100	−11.8	−16.4	−21.0	−16.0	−14.0	−4.6
150	−11.0	−16.5	−21.1	−15.6	−13.4	−3.9
200	−10.3	−16.6	−21.3	−15.2	−13.0	−3.2

Note. RCP = RCP=representative concentration pathway.

TABLE 9 Comparison of historical (1984–2013) and projected flow return periods for two future time periods (2036–2065 and 2066–2095) in Upper Campbell Lake reservoir, British Columbia, Canada

		Return period (year)					
		2036–2065			2066–2095		
Flow (m^3/s)	Historical	RCP 2.6	RCP 4.5	RCP 8.5	RCP 2.6	RCP 4.5	RCP 8.5
800	3	4	4	4	4	4	3
1000	5	8	8	10	8	8	6
1250	11	20	21	26	21	20	14
1500	22	40	45	57	45	42	28
1900	60	105	135	178	130	117	75

Note. RCP = RCP=representative concentration pathway.

6 | CONCLUSIONS AND SUMMARY

This study used multiple RCPs, GCMs, and DSMs to assess the uncertainty in streamflow due to climate change. The analyses are performed for the case study of Campbell River basin in BC, Canada, with the focus on Strathcona dam location. Most of the previous regional studies in Canada found that the choice of GCMs is the biggest source of uncertainty in downscaling processes. The analyses in the Campbell River basin performed with different RCPs, GCMs, and DSMs show that the choice of DSMs has a higher influence on streamflow variation compared to the choice of GCMs or RCPs. DSMs are developed based on a statistical relationship between climate variables. DSMs includes multiple assumptions, selections of statistical parameters (e.g., scale, shape, and skewness), and climate variables (predictand and predictors), which make a DSM different from other DSMs. Therefore, structure and procedure followed in a DSM could be possible reasons for significant streamflow variation for various DSMs. Hence, it is important to use multiple DSMs during climate change impact assessment. Mandal et al. (2016a) reached a similar conclusion in the study of Pr projection under changing climatic conditions. It is to be expected that if the Pr pattern is affected, then the streamflow will change too. However, the previous study, Mandal et al. (2016a) does not quantify the amount of Pr or future streamflow changes. According to Warren and Lemmen (2014), an increasing trend in average annual Pr can be found on the west coast of Canada where snowfall has decreased in last 61 years (1950 to 2010). Therefore, quantifying changes in streamflow due to climate change is an important contribution of this study that makes it different from the previous work. Another important difference of this study is the analysis of propagation of sources of uncertainty in the projected streamflow, which is discussed in Section 5.

From Table 7, it can be found that all the DSMs show similar pattern, for example, increasing trend in streamflow for winter and a decreasing trend for other seasons except KR and BR. However, KR agrees with summer and winter flow trend with other DSMs where BR captures streamflow pattern for all seasons except winter. BR and KR models are regression based, and multiple predictors variables (Tmax, Tmin, mslp, hus at 500 hPa, u-wind, and v-wind) are used to build a relationship between predictors and predictand (here Pr). These predictor variables are correlated with each other (positive or negative; Mandal et al., 2016b), which could be the reason for disagreement between KR and BR results when compared with other DSMs.

For the purpose of this study, a single hydrologic model (UBCWM) is used which is an obsolete model and a limitation of this study at this stage. The selection of hydrologic models depends upon the study region, data availability, basin characteristics, and study purposes but often the model is selected, which is readily available. In this case, BC Hydro provided the calibrated model (UBCWM). In addition, Kay et al., (Kay et al., 2009) investigated the role of different hydrologic models and found that the choice of the hydrologic model also contributes to the uncertainty in projected streamflow. Also, projected streamflow is highly sensitive to hydrologic model parameterization (Jiang et al., 2007; Poulin, Brissette, Leconte, Arsenault, & Malo, 2011). However, it has been found that uncertainty due to the hydrological model structure is more significant compared to model parameter uncertainty. Therefore, streamflow generation using multiple

hydrological models with multiple RCPs, GCMs, and DSMs may be advised for the continuation of the presented work. There are two other dams in the basin (Ladore and John Hart) that are connected with the Strathcona dam. Hence, quantifying stream flow uncertainty due to climate change at all three dam locations could be another area of future research. Another limitation of the study is the use of a single river catchment. The consistency of GCMs varies substantially from one region to another. Rupp, Abatzoglou, Hegewisch, and Mote (2013) and Kay et al. (2009) also suggested that multiple catchments, or different locations, should be analyzed in order to obtain a more comprehensive understanding of different sources of uncertainty. Focus of the present work is in the development of the uncertainty assessment methodology that can be used with multiple catchments for more thorough analyses of uncertainty. This work is considered as a potential future research topic. In this study, only four GCMs are used due to data availability for all DSMs. GCMs use mathematical relationships to simulate global climate system in three spatial dimensions with respect to time. GCMs simulate different atmospheric components (temperature, sea ice, and humidity) at various scales (horizontal spacing and grid size) and include many complexities (parameterization schemes). Some GCMs are based on the same analytical procedures and even share the same mathematical equations. Therefore, future climate predictions using an arbitrary number of GCMs may be very precise and consistent for a particular region, but it may be inaccurate as the outcome can be consistently biased. For example, Rupp et al. (2013) found that two GCMs, MIROC-ESM-CHEM and MIROC-ESM, to perform poorly in Europe and Southeast Asia. However, these two models perform well in Africa. Therefore, selection of GCMs is crucial for uncertainty analysis and may be a potential future research area.

Another main observation of the presented study is that the winter flow will be increasing in both future time periods considered (2036–2065 and 2065–2095), where the summer flow will be decreasing by atleast 21%. These findings can have a serious effect on the management of water resources infrastructure in the basin, which is one of the main components of the BC hydropower generation system. However, a major weakness of river flow forecast under climate change is limited validation. There is a prospect for testing the primary flow patterns relative to recent empirical trends, which provide an opportunity for future work. The recommendations of the study presented in this paper are as follows: (a) the new water resources infrastructure planning and design guidelines should be developed in order to include the changing climatic conditions in the future and (b) the serious review of the current operational rules for the water resources infrastructure in the basin should be conducted in with the main goal of finding the best adaptation strategies to changing future conditions.

ACKNOWLEDGMENTS

The work presented here is supported by Discovery Grant from the Natural Sciences and Engineering Council (NSERC) of Canada awarded to the second author. We extend our gratitude to BC Hydro for providing calibrated hydrological model and observed data for Campbell River system.

REFERENCES

Asokan, S. M., & Dutta, D. (2008). Analysis of water resources in the Mahanadi River basin, India under projected climate conditions. *Hydrological Processes*, *22*, 3589–3603. https://doi.org/10.1002/hyp.6962

BC Hydro Generation Resource Management. (2012). Campbell River system water use plan. Available at: http://www.bchydro.com/content/dam/hydro/medialib/internet/documents/planning_regulatory/wup/vancouver_island/2012q4/campbell_river_WUP_accept_2012_11_21.pdf [Accessed 12 March 2015].

Bürger, G., Sobie, S. R., Cannon, A. J., Werner, A. T., & Murdock, T. Q. (2012). Downscaling extremes: An Intercomparison of multiple methods for future climate. *Journal of Climate*, *26*, 3429–3449. https://doi.org/10.1175/JCLI-D-12-00249.1

Canadian Council of Professional Engineers. (2008). Adapting to climate change: Canada's first national engineering vulnerability assessment of public infrastructure. Available at: http://www.pievc.ca/e/Adapting_to_climate_Change_Report_Final.pdf [Accessed 4 July 2016].

Canadian Institute of Actuaries. (2014). Water damage risk and Canadian property insurance pricing. Available at: http://www.cia-ica.ca/docs/default-source/2014/214020e.pdf [Accessed 4 July 2016].

Craig, J. R., & Snowdon, A. P. (2010). Raven: A rigorously formalized modular hydrological model. *Environmental Modelling and Software*, *2*(20), Available at: http://www.civil.uwaterloo.ca/jrcraig/Raven/files/RavenManual_v2.6.pdf

Das, S., Millington, N., & Simonovic, S. P. (2013). Distribution choice for the assessment of design rainfall for the city of London (Ontario, Canada) under climate change. *Canadian Journal of Civil Engineering*, *40*(2), 121–129. https://doi.org/10.1139/cjce-2011-0548

Das, S., & Simonovic, S. P. (2012). Assessment of uncertainty in flood flows under climate change: The Upper Thames River basin (Ontario, Canada). Department of Civil and Environmental Engineering, University of Western Ontario, London, Ontario. Available at: http://www.eng.uwo.ca/research/iclr/fids/publications/products/79.pdf [Accessed 20 April 2014].

Dibike, Y. B., & Coulibaly, P. (2005). Hydrologic impact of climate change in the Saguenay watershed: Comparison of downscaling methods and hydrologic models. *Journal of Hydrology*, *307*(1–4), 145–163. https://doi.org/10.1016/j.jhydrol.2004.10.012

Eum, H., Simonovic, S. P., & Kim, Y. (2010). Climate change impact assessment using K-nearest neighbor weather generator: Case study of the Nakdong River basin in Korea. *Journal of Hydrologic Engineering*, *15*(10), 772–785. https://doi.org/10.1061/(ASCE)HE.1943-5584.0000251

Fowler, H. J., & Wilby, R. L. (2010). Detecting changes in seasonal precipitation extremes using regional climate model projections: Implications for managing fluvial flood Risk. *Water Resources Research*, *46*(3), 1–17. https://doi.org/10.1029/2008WR007636

Heffernan, J. E. (2016). An introduction to statistical modeling of extreme values: 1–33. Available at: http://www.ral.ucar.edu/~ericg/softextreme.php [Accessed 30 August 2016].

Hosking, J. R. M., & Wallis, J. R. (1997). *Regional frequency analysis: An approach based on L-moments*. New York: United States of America by Cambridge University Press Available at: https://books.google.com.pe/books?hl=es&lr=&id=gurAnfB4nvUC&oi=fnd&pg=PP1&dq=Regional+frequency+analysis+an+approach+based+on+l-moments&ots=7Re17uu4PZ&sig=cQloBXfu6O-1BS3wGAj_pUvSJYI#v=onepage&q&f=false [Accessed 30 September 2016].

Hutchinson, M. F., & Xu, T. (2013). Anusplin version 4.4 user guide. (August) Available at: http://fennerschool.anu.edu.au/files/anusplin44.pdf [Accessed 2 May 2016].

IPCC (2013). *Climate change 2013: The physical science basis. Contribution of working group I to the fifth assessment report of the Intergovernmental panel on climate change*. Cambridge, United Kingdom and New York, NY, USA: Cambridge University Press 1535 pp.

Irwin, S., Srivastav, R. K., Simonovic, S. P., & Burn, D. H. (2016). Delineation of precipitation regions using location and atmospheric variables: The role of attribute selection. *Hydrological Sciences Journal*, *62*(2). https://doi.org/10.1080/02626667.2016.1183776

Jiang, T., Chen, Y. D., Xu, C. Y., Chen, X., Chen, X., & Singh, V. P. (2007). Comparison of hydrological impacts of climate change simulated by six hydrological models in the Dongjiang Basin, South China. *Journal of Hydrology*, *336*(3–4), 316–333. https://doi.org/10.1016/j.jhydrol.2007.01.010

Kannan, S., & Ghosh, S. (2013). A nonparametric kernel regression model for downscaling multisite daily precipitation in the Mahanadi basin. *Water Resources Research*, *49*, 1360–1385. https://doi.org/10.1002/wrcr.20118

Kay, A. L., Davies, H. N., Bell, V. A., & Jones, R. G. (2009). Comparison of uncertainty sources for climate change impacts: Flood frequency in England. *Climatic Change*, *92*, 41–63. https://doi.org/10.1007/s10584-008-9471-4

King, L. M., Mcleod, I. A., & Simonovic, S. P. (2015). Improved weather generator algorithm for multisite simulation of precipitation and temperature. *Journal of the American Water Resources Association*, *7*, 1–16. https://doi.org/10.1111/1752-1688.12307

Leclerc, M., & Ouarda, T. B. M. J. (2007). Non-stationary regional flood frequency analysis at ungauged sites. *Journal of Hydrology*, *343*(3–4), 254–265. https://doi.org/10.1016/j.jhydrol.2007.06.021

Mandal, S., Breach, P. A., & Simonovic, S. P. (2016a). Uncertainty in precipitation projection under changing climate conditions: A regional case study. *American Journal of Climate Change*, *5*(1), 116–132. https://doi.org/10.4236/ajcc.2016.51012

Mandal, S., Srivastav, R. K., & Simonovic, S. P. (2016b). Use of beta regression for statistical downscaling of precipitation in the Campbell River basin, British Columbia, Canada. *Journal of Hydrology*, *538*, 49–62. https://doi.org/10.1016/j.jhydrol.2016.04.009

McCuen, R. H. (2016). Assessment of hydrological and statistical significance. *Journal of Hydrologic Engineering*, *21*(4) 2516001. https://doi.org/10.1061/(ASCE)HE.1943-5584.0001340

Micovic, Z., & Quick, M. C. (1999). A rainfall and snowmelt runoff modelling approach to flow estimation at ungauged sites in British Columbia. *Journal of Hydrology*, *226*(1–2), 101–120. https://doi.org/10.1016/S0022-1694(99)00172-9

Micovic, Z., & Quick, M. C. (2009). Investigation of the model complexity required in runoff simulation at different time scales/Etude de la complexité de modélisation requise pour la simulation d'écoulement à différentes échelles temporelles. *Hydrological Sciences Journal*, *54*(5), 872–885. https://doi.org/10.1623/hysj.54.5.872

Najafi, M. R., Moradkhani, H., & Jung, I. W. (2011). Assessing the uncertainties of hydrologic model selection in climate change impact studies. *Hydrological Processes*, *25*(18), 2814–2826. https://doi.org/10.1002/hyp.8043

Pacific Climate Impacts Consortium U of V. (2014). Statistically downscaled climate scenarios. Available at: https://pacificclimate.org/data/statistically-downscaled-climate-scenarios [Accessed 23 July 2015].

Poulin, A., Brissette, F., Leconte, R., Arsenault, R., & Malo, J.-S. (2011). Uncertainty of hydrological modelling in climate change impact studies in a Canadian, snow-dominated river basin. *Journal of Hydrology*, *409*(3–4), 626–636. https://doi.org/10.1016/j.jhydrol.2011.08.057

Prudhomme, C., & Davies, H. (2008). Assessing uncertainties in climate change impact analyses on the river flow regimes in the UK. Part 1: Baseline climate. *Climatic Change*, *93*, 177–195. https://doi.org/10.1007/s10584-008-9464-3

Quick, M. C., & Pipes, A. (1977). U.B.C. WATERSHED MODEL/Le modèle du bassin versant U.C.B. *Hydrological Sciences Bulletin*, *22*(1), 153–162. https://doi.org/10.1080/02626667709491701

Refsgaard, J. C. (1997). Parameterisation, calibration and validation of distributed hydrological models. *Journal of Hydrology*, *198*(1–4), 69–97. https://doi.org/10.1016/S0022-1694(96)03329-X

Rupp, D. E., Abatzoglou, J. T., Hegewisch, K. C., & Mote, P. W. (2013). Evaluation of CMIP5 20th century climate simulations for the Pacific Northwest USA. *Journal of Geophysical Research: Atmospheres*, *118*(19), 10,884–10,906. https://doi.org/10.1002/jgrd.50843

Schnorbus M, Bennett A, Werner A, Berland A. 2011. Hydrologic impacts of climate change in the Peace, Campbell and Columbia watersheds, British Columbia, Canada. Available at: https://pacificclimate.org/sites/default/files/publications/Schnorbus.HydroModelling.FinalReport2.Apr2011.pdf [Accessed 10 Feb 2016].

Simonovic, S. P. (2008). Engineering literature review: Water resources—Infrastructure impacts, vulnerabilities and design considerations for future climate change. In Adapting to Climate Change, Canada's First National Engineering Vulnerability Assessment of Public Infrastructu. https://doi.org/10.1017/CBO9781107415324.004

Srivastav, R. K., Schardong, A., & Simonovic, S. P. (2014). Equidistance quantile matching method for updating IDFCurves under climate change. *Water Resources Management*, *28*, 2539–2562. https://doi.org/10.1007/s11269-014-0626-y

Srivastav, R. K., & Simonovic, S. P. (2014). Multi-site, multivariate weather generator using maximum entropy bootstrap. *Climate Dynamics*. https://doi.org/10.1007/s00382-014-2157-x

Surfleet, C. G., & Tullos, D. (2013). Uncertainty in hydrologic modelling for estimating hydrologic response due to climate change (Santiam River, Oregon). *Hydrological Processes*, *27*, 3560–3576. https://doi.org/10.1002/hyp.9485

US Army Corps of Engineers. (2000). Hydrologic modeling system HEC-HMS technical reference manual. doi:CDP-74B

van Vuuren, D. P., Edmonds, J., Kainuma, M., Riahi, K., Thomson, A., Hibbard, K., … Rose, S. K. (2011). The representative concentration pathways: An overview. *Climatic Change*, *109*(1), 5–31. https://doi.org/10.1007/s10584-011-0148-z

Warren, F. J., & Lemmen, D. S. (2014). Canada in a changing climate:Sector perspectives on impacts and adaptation. Government of Canada, Ottawa, ON, 286p.

Werner, A. T. (2011). BCSD downscaled transient climate projections for eight select GCMs over British Columbia, Canada. Hydrologic Modelling Project Final Report (Part I). Available at: http://scholar.google.com/scholar?hl=en&btnG=Search&q=intitle:BCSD+Downscaled+Transient+Climate+Projections+for+Eight+Select+GCMs+over+British+Columbia,+Canada#0%5Cnhttp://scholar.google.com/scholar?hl=en&btnG=Search&q=intitle:BCSD+downscaled+transient+cl [Accessed 17 September 2016].

Werner, A. T., & Cannon, A. J. (2015). Hydrologic extremes—An intercomparison of multiple gridded statistical downscaling methods. *Hydrology and Earth System Sciences Discussions*, *12*(6), 6179–6239. https://doi.org/10.5194/hessd-12-6179-2015

Wood, A. W., Leung, L. R., Sridhar, V., & Lettenmaier, D. P. (2004). Hydrologic implications of dynamical and statistical approaches to downscaling climate model outputs. *Climatic Change*, *62*, 189–216. https://doi.org/10.1023/B:CLIM.0000013685.99609.9e

Wood, A. W., Maurer, E. P., Kumar, A., & Lettenmaier, D. P. (2002). Long-range experimental hydrologic forecasting for the eastern United States. *Journal of Geophysical Research : Atmospheres*, *107*, 1–15. https://doi.org/10.1029/2001JD000659

How to cite this article: Mandal S, Simonovic SP. Quantification of uncertainty in the assessment of future streamflow under changing climate conditions. *Hydrological Processes*. 2017;31:2076–2094. https://doi.org/10.1002/hyp.11174

APPENDIX

BRIEF DESCRIPTION OF DOWNSCALING METHODS

A.1 | Bias-corrected spatial disaggregation (BCSD)

BCSD is a gridded downscaling method and efficiently used for downscaling GCM output (Werner, 2011; Werner & Cannon, 2015; Wood, Leung, Sridhar, & Lettenmaier, 2004). BCSD follows three steps: At first, monthly GCM simulated data is bias corrected using observed gridded data at GCM grid scale. Quantile mapping approach is used for the bias correction. In the next step, bias corrected monthly climate data is downscaled using interpolation at each local station and multiplied by a scaled factor. This step is called "local scaling," and the scale factor removes long term bias between observed and simulated climate variable. The following equation is used for local scaling process:

$$P_{ds}(x,t) = P_{\mathrm{mod}}(x,t)\frac{\langle P_{obs}\rangle_{mon}}{\langle P_{\mathrm{mod}}\rangle_{mon}}, \tag{A1}$$

where $P_{\mathrm{mod}}(x,t)$ is GCM simulated coarsely gridded monthly averaged climate variable at location x and t is a time in months "mon"; $P_{ds}(x,t)$ is downscaled monthly climate variable; and $\langle ...\rangle_{mon}$ is monthly mean of climate variable over the calibration period. In the final step, daily time series is generated from monthly mean climate data set using stochastic resampling technique (Wood, Maurer, Kumar, & Lettenmaier, 2002).

A.2 | Bias correction constructed analogues with quantile mapping reordering (BCCAQ)

BCCAQ is a hybrid gridded downscaling method which combines bias-corrected climate imprint and bias correction constructed analogues (BCCA) where bias-corrected climate imprint is cited as "inverse BCSD"(Werner & Cannon, 2015). BCCA adopts quantile mapping as a bias correction method and same spatial aggregation as BCSD, but it considers information from daily GCM anomalies instead monthly.

A.3 | K-nearest neighbor weather generator (K-NN CAD V4)

K-NN CAD V4 is a nonparametric multisite weather generator based on K-nearest neighbors (K-NN; King et al., 2015). It is an updated version of K-NN CAD V3 (Eum, Simonovic, & Kim, 2010) where block resampling and perturbation technique were introduced. The mathematical description of perturbation process is as follows:

$$y^{j}_{ppt,t+i} = \lambda_{ppt}x^{j}_{ppt,t+i} + (1-\lambda_{ppt})zt + i; i = 1,2,....n, \tag{A2}$$

where $y^{j}_{ppt,t+i}$is the perturbed precipitation value for t + t th day in jth location and t is current day; λ_{ppt} value varies in between 0 to 1 (0 means data series are totally perturbed and 1 means no perturbation in the results); $x^{j}_{ppt,t+i}$ is reshuffled nonzero precipitation value for $t + i$th day in jth location; and Z_{t+i}comes from two parameters log-normal distribution.

This model can preserve statistical features of observed historical climate variables with historical extremes.

A.4 | Maximum entropy bootstrap based weather generator (MEBWG)

MEBWG is a nonparametric multisite, multivariate weather generator developed by Srivastav and Simonovic (2014). This method consists of three main steps: (1) orthogonal transformation of spatially correlated climate variables at different locations; (2) generation of synthetic replications of climate variables using maximum entropy bootstrap (MEB); and (3) apply an inverse orthogonal transformation of synthetic climate variables to restore spatial correlation. Using the following equations, maximum entropy density is constructed:

$$m_1 = 0.75O_1 + 0.25O_2, \tag{A3}$$

$$m_k = 0.25O_{k-1} + 0.5O_k + 0.25O_{k+1}; \forall k = 2,3,....,t-1, \tag{A4}$$

$$m_t = 0.25O_{t-1} + 0.75O_t, \tag{A5}$$

where t is time step and O_t is rank matrix derived from the principal component analysis.

These above equations satisfy ergodic theorem (mean preserving). This method is free of modeling parameters and computationally inexpensive.

A.5 | Nonparametric multivariate kernel regression (KR) model

A multivariate multisite nonparametric KR model was developed by Kannan and Ghosh (2013). This model first projects precipitation states of the study area using classification and regression trees. In the final step, the model simulates multisite precipitation amounts conditioned on the estimated precipitation states using KR. The general form of KR's conditional expectation can be formulated as follows:

$$E(Y/X) = m(X) = \frac{\int yf(y/x)}{f_x(x)}, \tag{A6}$$

where Y is the simulated precipitation; X is principal component of the predictor variables; $f(y/x)$ is conditional probability density function (pdf) of Y given X = x; and $f_x(x)$ is marginal pdf of X.

In the downscaling model, the pdf in Equation A6 is replaced by kernel density estimator and expressed as follows:

$$m_h(x) = \frac{\sum_{i=1}^{n} K_h(x-X_i)Y_i}{\sum_{i=1}^{n} K_h(x-X_i)}, \tag{A7}$$

where $m_h(x)$ the expected is value Y for a condition of $X_i = x$ and K_h is the kernel with bandwidth h. This method was first successfully applied at eight different locations in the Mahanadi river basin, India.

A.6 | Multisite and multivariate beta regression (BR) model

A multisiteBR-based downscaling method was proposed by Mandal et al. (2016b). BR model simulates precipitation at multiple locations conditioned on precipitation states. This model integrates an unsupervised clustering technique (K-means), classification and

regression trees, principal component analysis and BR. The BR model works in two phases. In the first phase, it predicts precipitation states of a catchment, and in final step, it simulates future precipitation based on precipitation states. Large-scale climate variables, for example, daily maximum and minimum air surface temperature, mslp, hus at 500 hPa, zonal (u-wind), and meridional (v-wind) wind are used as predictor variables for this model to predict precipitation. The generalized mathematical formulation of BR model is given as follows:

$$P_t = F_R(X_t/S_t), \tag{A8}$$

where P_t is the simulated precipitation at a certain location at time t, X_t is predictor variables, and S_t is precipitation state of the catchment.